Anomalous Thermal Transport in Silicon-Like Nanowires with One-Dimensional Correlated Disorder

Wei Zhang(张薇)[1,2], Shiyun Xiong(熊世云)[3*], Yangyu Guo(郭洋裕)[1,2], Hongliang Yi(易红亮)[1,2*], Masahiro Nomura[4], and Sebastian Volz[4,5]

[1]*School of Energy Science and Engineering, Harbin Institute of Technology, Harbin 150001, China*
[2]*Key Laboratory of Aerospace Thermophysics, Ministry of Industry and Information Technology, Harbin 150001, China*
[3]*Guangzhou Key Laboratory of Low-Dimensional Materials and Energy Storage Devices, School of Materials and Energy, Guangdong University of Technology, Guangzhou 510006, China*
[4]*Institute of Industrial Science, The University of Tokyo, Tokyo 153-8505, Japan*
[5]*Laboratory for Integrated Micro and Mechatronic Systems, CNRS-IIS UMI 2820, The University of Tokyo, Tokyo 153-8505, Japan*

(Received 19 August 2025; accepted manuscript online 3 November 2025)

Understanding how structural disorder affects phonon transport is critical for controlling thermal conduction in nanoscale materials. In this work, we investigate thermal transport in Si-like nanowires composed of layered atoms with one-dimensional correlated disorder. Using the nonequilibrium Green's function method, we reveal that introducing correlation among atomic layers induces phonon Anderson localization at low-frequencies, leading to a nonmonotonic length dependence of thermal conductivity: it increases at short lengths but decreases beyond a critical size, in sharp contrast to the monotonic trend observed in random disorder. Despite having fewer mass interfaces, the correlated nanowires exhibit lower thermal conductivity than their random disorder counterparts when the nanowire length exceeds 70 nm. Frequency-resolved analysis shows that spatial correlation suppresses the transmission of low-frequency phonons and promotes their localization, while concurrently extending the localization length of mid- and high-frequency modes. This selective reshaping of phonon localization is responsible for the anomalous transport behavior. Our findings provide new insights into heat transport engineering via tailored disorder in low-dimensional materials.

DOI: 10.1088/0256-307X/42/12/120804 CSTR: 32039.14.0256-307X.42.12.120804

1. Introduction. Heat transport in nanoscale materials plays a central role in a wide range of technologies, including thermoelectric energy conversion,[1,2] thermal insulation,[3] and thermal rectification.[4–6] Unlike their bulk counterparts, nanoscale systems exhibit transport characteristics that deviate significantly from the predictions of Fourier's law, owing to the prominent role of size effects, interface scattering, and wave interference phenomena.[7–9] At reduced dimensions, the coherence and phase information of phonons are preserved over long distances, opening up new opportunities to manipulate heat flow through phononic band engineering,[10–15] structural disorder,[16–20] or topological design.[21,22]

In recent years, growing attention has been devoted to the role of phonon localization in low-dimensional thermal transport. Anderson localization, a phenomenon arising from wave interference due to multiple coherent scatterings, is known to suppress wave propagation in disordered media.[23–25] While originally proposed in the context of electronic systems, the localization has been extensively explored in phonon transport through harmonic chains,[26,27] aperiodic superlattices,[28–31] and random disordered nanostructures.[17,32–37] The hallmark of Anderson localization is an exponential decay of transmission with system length, resulting in saturation or even decrease of thermal conductivity at large length scales. However, in typical mass-disordered systems, low-frequency phonons tend to remain extended due to their long wavelengths and weak scattering rates, masking the localization signature in cumulative transport observables.

The extent to which phonon localization manifests is strongly influenced by the type and structure of disorder. Unlike atomic-scale point defects, multilayered disordered architectures allow for controlled variation in parameters such as mass contrast, interface density, and layer sequence, enabling systematic exploration of localization mechanisms. Disordered Si/Ge superlattices, for instance, have been shown to exhibit ultralow thermal conductivity and pronounced anisotropy due to strong phonon localization.[28] Numerical investigations based on mode-resolved nonequilibrium Green's function (NEGF) techniques have further confirmed that transmission decays exponentially in such structures, with well-defined localization lengths directly correlating with suppressed thermal transport.[29] Thermal resistance in random multilayers can also be enhanced by introducing an optimal degree of structural randomness, which increases local mismatch

*Corresponding authors. Email: syxiong@gdut.edu.cn; yihongliang@hit.edu.cn
© 2025 Chinese Physical Society and IOP Publishing Ltd. All rights, including for text and data mining, AI training, and similar technologies, are reserved.

and promotes coherent backscattering.[38] In graphene/h-BN heterostructures, the coexistence of aperiodic stacking and interfacial mixing leads to a substantial reduction in thermal conductivity, driven by enhanced phonon Anderson localization.[31] While these results underscore the potential of disordered multilayer systems to support phonon localization, they are largely confined to configurations with uncorrelated randomness, where each perturbation occurs independently.

Recently, correlated disorder structures have been illustrated to hinder thermal transport significantly. Correlated disorder is characterized by a nonzero correlation function between spatially separated perturbations, typically decaying as a power law with distance.[39] Recent studies have demonstrated that spatial correlations in structural disorder can profoundly influence phonon localization and thermal transport. The influence of such correlations has been investigated across a range of material platforms. For example, first-principles simulations on SiGe alloys reveal that introducing controlled spatial correlations in atomic mass distribution can significantly modify thermal conductivity, either enhancing or suppressing it depending on the correlation length.[40] Vibrational localization has also been observed to persist in systems with long-range interactions, where correlation-induced coherence plays a crucial role in sustaining non-diffusive energy transport.[27] Moreover, breaking the traditional Rayleigh scattering framework via engineered disorder correlations has been proposed as a strategy to manipulate phonon scattering rates beyond the capabilities of conventional models.[41] These findings highlight the emerging paradigm of disorder engineering, where spatial correlations are leveraged to manipulate phonon transport at the nanoscale. Despite these advances, most existing studies on correlated disorder have focused on either atomic-scale systems or continuous media, leaving open questions about how such effects manifest in discretely layered nanostructures. In particular, the role of spatially correlated mass disorder in quasi-one-dimensional multilayer systems has received limited attention.

In this work, we investigate phonon transport in one-dimensional (1D) nanowires with spatially correlated mass disorder. By employing the NEGF formalism, we systematically analyze the effects of disorder correlation on phonon transmission, localization length, and thermal conductivity across a wide range of system lengths. We find that correlation leads to a nonmonotonic dependence of thermal conductivity on length, which signifies the emergence of phonon Anderson localization. In particular, correlated disorder suppresses low-frequency phonon transmission more effectively than random disorder, despite having fewer mass interfaces. Our results demonstrate that spatial correlations within disorder can be leveraged to engineer thermal transport at different phonon frequencies, offering a powerful strategy for designing nanostructures with tunable heat conduction properties.

2. Methods.

2.1. Construction of 1D Correlated Disordered Nanowires.

We consider a Si-like nanowire with a cross section of 3.26 nm×3.26 nm, where the z-direction serves as the phonon transport direction. The term "Si-like" refers to the fact that the nanowire adopts the lattice structure, lattice constant, and interatomic force constants characteristic of crystalline silicon, while allowing for variations in atomic mass to simulate disorder. The atoms with the same z coordinate are identified as an atomic layer. Each atomic layer contains atoms of identical mass, while the mass value varies from layer to layer according to a one-dimensional correlated disordered sequence. This design results in a stratified nanowire composed of atomically flat mass layers.

To generate the correlated mass sequence, we adopt the improved Fourier filtering method, originally developed for modeling correlated percolation and disordered media.[42,43] Specifically, we generate a sequence of N continuous Gaussian random variables $\{\phi_z\}$ on a 1D lattice indexed by the layer position $z = 1, 2, \ldots, N$. These variables are power-law correlated, with a correlation function decaying as

$$\langle \phi_z \phi_{z+r} \rangle \sim r^{-a}, \tag{1}$$

where a is the correlation exponent. A smaller value of a indicates stronger correlation.

The structure generation proceeds as follows: we start by sampling uncorrelated Gaussian random numbers u_q in Fourier space with zero mean and unit variance. These are multiplied by the square root of the desired power-law spectral density $S(q)$ to obtain correlated Fourier coefficients,

$$\phi_q = \sqrt{S(q)}\, u_q. \tag{2}$$

An inverse discrete Fourier transform then yields the correlated real-space sequence $\{\phi_z\}$. We adopt the functional form,[39]

$$C(r) = (1 + r^2)^{-a/2}, \tag{3}$$

which avoids divergence at $r = 0$ while preserving the correct asymptotic decay. Figures 1(a) and 1(e) illustrate the correlation function $C(r)$ for $a = 0.1$ and $a = 1$, respectively.

To discretize the sequence for physical modeling, we map the continuous values ϕ_z to five discrete mass types by assigning them to equally sized quantiles of the cumulative distribution, as shown in Fig. 1. Specifically, each ϕ_z is mapped to an integer $s_z \in \{1, 2, 3, 4, 5\}$, which corresponds to atomic masses $m_z = \gamma_{s_z} m_0$, where $m_0 = 50$ amu is the reference mass and $\gamma = \{0.4, 0.7, 1.0, 1.3, 1.6\}$ are dimensionless scaling factors. As a result, the layered nanowire possesses a 1D spatially correlated mass distribution that is fully defined by the correlation exponent a. For comparison, we also construct control nanowires with purely random (uncorrelated) mass sequences, generated by random permutations of the same five mass types with equal probability. Throughout this work, the term "random disorder" is used to describe structures in which each atomic layer mass is assigned independently without correlation. To maintain consistency, we use the term random disorder uniformly in the following discussion.

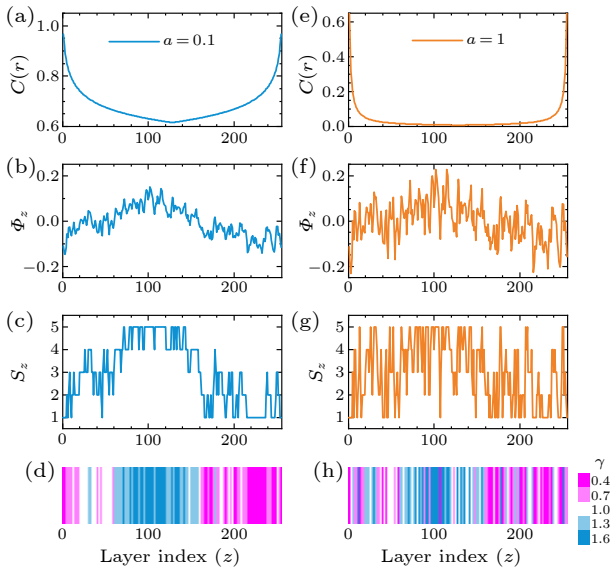

Fig. 1. Generation of one-dimensional correlated mass sequences for Si-like nanowires with correlation exponents (a)–(d) The correlation exponent $a = 0.1$ and (e)–(h) $a = 1$. Panels (a) and (e) are the target correlation function $C(r)$; (b) and (f) the Gaussian-correlated sequences ϕ_z; and (c) and (g) the discretized form s_z with five integers. Panels (d) and (h) display the resulting stratified nanowire structures, with layers color-coded by discrete mass scaling factors $\gamma \in \{0.4, 0.7, 1.0, 1.3, 1.6\}$.

2.2. Nonequilibrium Green's Function Method. The thermal conductivity of the constructed nanowires is computed using the NEGF formalism. The dynamical matrix of the nanowire is assembled from the interatomic force constants and mass distribution. The Tersoff empirical potential[44] for Si is adopted for force constants calculations. The system is coupled to two semi-infinite ideal leads (pristine Si nanowires), serving as thermal reservoirs. The phonon transmission function $\mathcal{T}(\omega)$ is calculated from the retarded/advanced Green's function $G^{\mathrm{r/a}}(\omega)$ of the central region and the self-energies of the leads,

$$\mathcal{T}(\omega) = \mathrm{Tr}[\Gamma_{\mathrm{L}} G^{\mathrm{r}} \Gamma_{\mathrm{R}} G^{\mathrm{a}}], \tag{4}$$

where $\Gamma_{\mathrm{L/R}}$ are the coupling matrices of the left/right leads.

With the derived transmission function, thermal conductivity is calculated based on the Landauer formula,[45–47]

$$\kappa = \frac{L}{S} \int_0^\infty \frac{\hbar\omega}{2\pi} \left(\frac{\partial f(\omega)}{\partial T}\right) \mathcal{T}(\omega) \mathrm{d}\omega, \tag{5}$$

where $f(\omega)$ is the Bose–Einstein distribution function. To ensure statistical reliability, S and L represent the cross-sectional area and the length of the central scattering region, respectively. Each result is averaged over five independent disordered mass sequence for a given a.

3. Results and Discussion. To investigate the impact of spatial correlation on phonon transport, we examine the thermal conductivity κ of silicon-like nanowires as a function of length L for different disorder types,

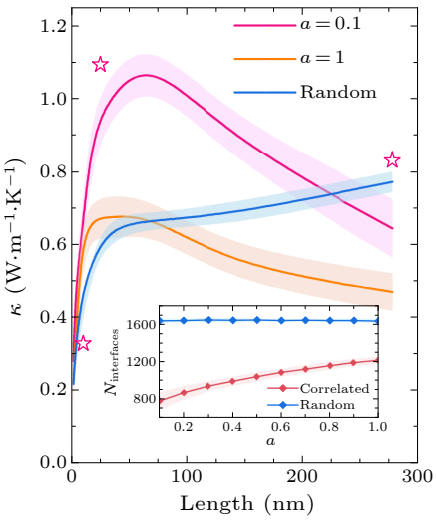

Fig. 2. Length-dependent thermal conductivity at 300 K for random disorder, weakly correlated disorder ($a = 1$) and strongly correlated disorder ($a = 0.1$). Shaded areas show standard deviation over five realizations. Magenta pentagrams denote the nonequilibrium molecular dynamics results for the correlated case of strongly correlated disorder ($a = 0.1$). The insert shows the number of interfaces in nanowires of length 278.1 nm as a function of the correlation exponent a.

as shown in Fig. 2. Although all results are presented at 300 K, the same qualitative behavior is expected at other temperatures. Within the harmonic Landauer NEGF framework, the phonon transmission is intrinsically temperature-independent, and the influence of temperature enters only through the Bose–Einstein weighting factor in the transport integral. Since phonon scattering in the correlated nanowires is dominated by structural disorder rather than anharmonic interactions, the overall temperature effect on transmission and localization is minimal. For each configuration, the thermal conductivity κ was averaged over five independent disorder realizations to account for statistical variability arising from finite sampling. The standard deviations across these realizations are shown as shaded regions in Fig. 2. For instance, at $L = 69.5$ nm, the standard deviation of κ is approximately $\pm 0.05\,\mathrm{W{\cdot}m^{-1}{\cdot}K^{-1}}$ for the correlated case with $a = 0.1$, and $\pm 0.04\,\mathrm{W{\cdot}m^{-1}{\cdot}K^{-1}}$ for $a = 1$. These uncertainty levels are small compared to the overall variation of κ with length and therefore do not affect the observed nonmonotonic trends or the comparison between different correlation strengths. Notably, the random nanowires exhibit slightly lower standard deviations, which can be attributed to their more homogeneous statistical distribution of atomic mass layers. For the random mass disorder, κ increases monotonically with length until 300 nm, a signature of non-diffusive transport. However, we observe that the growth rate of κ diminishes significantly beyond $L \approx 34.8$ nm. This sublinear increase can be attributed to the onset of multiple scattering events among mid- to high-frequency phonons, which gradually transit from ballistic transport to diffusive transport. In the ballistic transport regime, the thermal conductance remains constant, while

the thermal conductivity increases with system length. In contrast, in the diffusive regime, the thermal conductivity saturates and becomes length-independent, leading to a decrease in thermal conductance as the system length increases.

The introduction of spatial correlation into the mass disorder sequence fundamentally alters this trend. For weakly correlated disorder ($a = 1$), κ initially increases sharply with length when $L < 17.4\,\text{nm}$, showing a steeper slope than the random case. The initial enhancement is due to the reduced number of abrupt mass interfaces in correlated structures, which weakens short-range phonon scattering. Interestingly, for intermediate lengths ($17.4\,\text{nm} < L < 69.5\,\text{nm}$), κ becomes nearly flat, suggesting a saturation regime where additional increase in system length no longer improves heat transport. More strikingly, at larger lengths ($L > 69.5\,\text{nm}$), κ begins to decrease with increasing L, and ultimately becomes lower than the corresponding randomly disordered nanowires, which is a signature of phonon Anderson localization. The observed results suggest that although spatial correlation suppresses short-range scattering by reducing the number of interfaces, it also introduces structural modulations that enhance coherent backscattering and drive phonon localization at larger length scales.

The inset of Fig. 2 provides further insight by comparing the number of interfaces for different correlation exponents at $L = 278.1\,\text{nm}$. As expected, random nanowires exhibit the highest number of interfaces, while correlated nanowires show significantly fewer interfaces. According to conventional phonon scattering theory, a greater number of interfaces should increase the probability of phonon scattering, thereby reducing thermal conductivity. However, our results challenge this paradigm. Although the correlated nanowires contain fewer interfaces, their thermal conductivity is lower than that of random ones at large L, due to the occurrence of Anderson localization induced by structural correlations, particularly for $a = 1$.

To test the robustness of the anomalous behavior, we further compute $\kappa(L)$ for nanowires with stronger correlation ($a = 0.1$). Additional simulations for other correlation exponents ($a = 0.001$, 0.01, and 2) are also performed, and similar thermal conductivity peaks were found [Fig. S1 of the Supplementary Materials (SM)]. The inset of Fig. 2 shows that their interface count is even less, only about half that of the random case at the same length. As shown in Fig. 2, due to the reduced number of interfaces, κ increases even more sharply with length compared to the case of $a = 1$. The peak κ reaches $1.05\,\text{W}\cdot\text{m}^{-1}\cdot\text{K}^{-1}$ at $L = 69.5\,\text{nm}$, after which κ rapidly decreases. The reduction rate of κ with length in system with $a = 0.1$ after the peak is also much rapid than the case with $a = 1$, indicating a stronger Anderson localization in stronger correlated systems.

These observations collectively demonstrate that phonon scattering at short-range mass interfaces is not the dominant mechanism suppressing heat transport in these correlated systems. Instead, the correlations do not scatter phonons in the traditional incoherent sense but promote coherent back-scattering, giving rise to phonon Anderson localization. In such a regime, phonons become localized to finite spatial regions with exponentially decaying wavefunctions, leading to a reduction in the number of thermally active phonon modes and an overall decline in κ as system length increases. The results in correlated disordered structures reveal a breakdown of the traditional interface-scattering framework, which demonstrates reduced thermal conductivity with intensified interfaces. Although the system contains fewer interfaces, which are ostensibly favorable for phonon propagation, correlated nanowires exhibit lower thermal conductivity than their random counterparts at sufficient lengths. This counterintuitive behavior arises because long-range structural correlations promote coherent backscattering and phonon localization, rather than simple interface scattering, thereby suppressing thermal conductivity even with fewer interfaces. For comparison, we calculated the thermal conductivity of a pristine Si nanowire with the same $3.26 \times 3.26\,\text{nm}^2$ cross section. The value is approximately $9.0\,\text{W}\cdot\text{m}^{-1}\cdot\text{K}^{-1}$ at a length of $\sim$50 nm and increases to about $16.0\,\text{W}\cdot\text{m}^{-1}\cdot\text{K}^{-1}$ at $\sim$200 nm, which are in agreements with previous reports.[48] These values are more than an order of magnitude higher than those of the disordered nanowires, reflecting the pronounced suppression of phonon transport induced by mass disorder.

To understand the frequency-dependent contributions to κ, we compute the accumulative thermal conductivity $\kappa_{\text{accu}}(\omega)$ for different lengths and disorder types. Figures 3(a)–3(c) show the results for random disorder, weakly correlated ($a = 1$), and strongly correlated ($a = 0.1$) nanowires, respectively. In the random case, thermal transport is heavily dominated by low-frequency phonons, as shown in Fig. 3(a). At short length ($L = 17.4\,\text{nm}$), phonons with $\omega < 5\,\text{THz}$ contribute over 85% of the total thermal conductivity. As the system becomes longer, mid- and high-frequency phonons increasingly suffer from multiple scattering at the numerous mass interfaces. By $L = 278.1\,\text{nm}$, more than 85% of the thermal conductivity is carried by phonons below 1 THz. This progressive suppression of higher-frequency modes leads to a narrowing of the thermally active spectral window as the length of the nanowires increase. The introduction of correlation modifies this trend in nontrivial ways. For weakly correlated disorder ($a = 1$) [Fig. 3(b)], the contribution from mid-frequency phonons becomes more significant, especially at longer lengths. At $L = 278.1\,\text{nm}$, the frequency range required to reach 85% of κ broadens to approximately 2 THz. Strikingly, for strongly correlated disorder ($a = 0.1$), the effective thermal transport window extends even further, as shown in Fig. 3(c). At $L = 278.1\,\text{nm}$, phonons up to nearly 4.5 THz contribute 85% of the thermal conductivity. The further broadening suggests that in correlated structures, mid-frequency phonons contribute more significantly to thermal transport because correlation leads to fewer and weaker mass interfaces along the transport direction, thereby reducing phonon scattering.

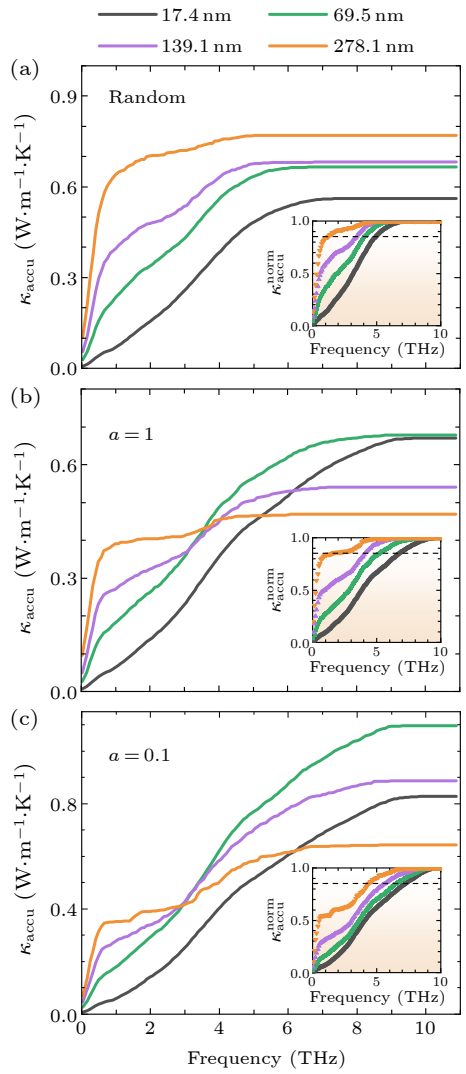

Fig. 3. Accumulative thermal conductivity $\kappa_{\mathrm{accu}}(\omega)$ for nanowires with different lengths and (a) random disorder, (b) weakly correlated disorder ($a = 1$), and (c) strongly correlated disorder ($a = 0.1$). Insets show normalized cumulative κ versus frequency.

The above results demonstrate that randomly distributed interfaces primarily scatter mid-to-high frequency phonons, while correlated structures weakens the scattering of mid-to-high frequency modes due to the reduced interfaces but hinders low-frequency phonon transport by generating localizations.

However, the broadening of spectral contribution does not ensure an enhancement in overall κ. As shown earlier in Fig. 2, the total thermal conductivity in correlated systems is lower at large L despite the broader frequency participation. This apparent contradiction is resolved by recognizing that in layered disordered nanowires, correlations induce extended fluctuations that form effective barriers or potential wells for phonons. While low-frequency phonons are generally less susceptible to scattering due to their long wavelengths, in correlated structures they can experience coherent back-scattering across large scales, leading to Anderson localization even at low frequencies. At the same time, high-frequency phonons, whose wavelengths are comparable to the interlayer spacing, are inherently sensitive to any layer-to-layer mass variation. In random disorder systems, this leads to strong scattering and localization. In correlated systems, the number of interfaces is dramatically reduced, leading to the weakening of mid-to-high frequency phonon scattering and enhanced thermal transport for these modes. However, their contribution is not sufficient to offset the thermal conductivity suppression of low-frequency phonon induced by localization. As a result, the overall thermal conductivity decreases with increasing length, particularly in the strongly correlated case. Therefore, we illustrate a fundamental shift in the spectral nature of heat transport: from low-frequency dominated conduction in random systems to broader but less efficient multi-frequency transport in correlated systems. The redistribution, rather than helping heat transport, actually signals the progressive collapse of non-localized channels, reinforcing the picture of correlation-induced Anderson localization as the dominant mechanism suppressing κ at large scales.

To further elucidate the mechanism underlying the suppressed thermal conductivity in correlated disorder nanowires, we examine the frequency-resolved phonon transmission $\mathcal{T}(\omega)$ at the low-frequency region, as shown in Fig. 4. For the random disorder nanowires, long-wavelength phonons are difficult to scatter due to their large wavelengths. As a result, phonons with frequencies below 0.6 THz exhibit nearly ballistic transport up to $L = 69.5$ nm, with transmission close to four. Even as the length increases to $L = 278.1$ nm, their transmission shows only a modest decline, indicating that these low-frequency modes remain largely unaffected by the random mass interfaces and continue to dominate thermal transport.

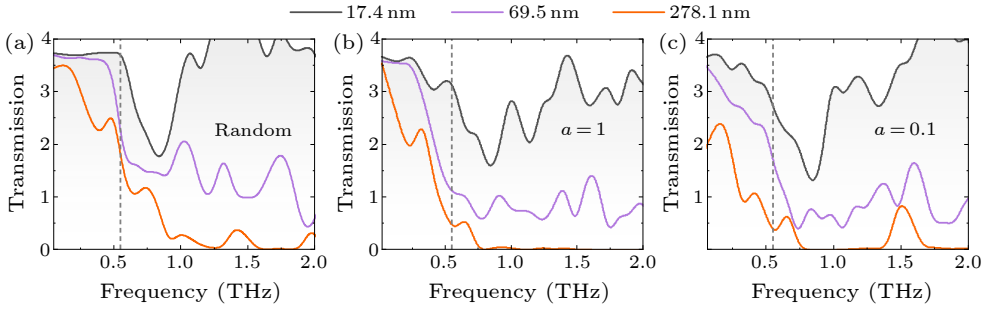

Fig. 4. Phonon transmission spectra below 2 THz for nanowires of different lengths and disorder types: (a) random, (b) $a = 1$, and (c) $a = 0.1$.

In contrast, both correlated systems ($a = 1$ and $a = 0.1$) show clear suppression of low-frequency transmission, particularly for $\omega < 0.6$ THz. Surprisingly, even though these structures contain significantly fewer mass interfaces (inset of Fig. 2), the transmission of low-frequency modes is markedly lower than in the random case. It reveals that correlations introduce extended spatial modulations in the mass distribution, which act as coherent scattering fields capable of localizing low-frequency phonons through interference effects. Moreover, stronger correlation (smaller a) leads to even more pronounced suppression of low-frequency transmission. For $a = 0.1$, the transmission exhibits exponential decline and overall lower values throughout the sub-THz range. This aligns with the results in Fig. 2, where the thermal conductivity for $a = 0.1$ shows a nonmonotonic trend and eventually falls below that of the random system at large lengths ($L > 200$ nm). It also explains the spectral redistribution observed in Fig. 3(c): the diminished low-frequency contribution is partially compensated by mid- and high-frequency modes, which are, however, not sufficient to recover the lost thermal conductivity.

As presented in Fig. 5, we compare the frequency-dependent transmission for random disorder nanowires and correlated systems with $a = 1$ and $a = 0.1$, at increasing lengths $L = 17.4$ nm to 278.1 nm. For random disorder, we observe that as the length increases, the transmission of high-frequency phonons ($\omega > 6$ THz) rapidly diminishes and becomes nearly zero when $L > 69.5$ nm. This indicates that these modes are strongly scattered by the dense and disordered mass interfaces and become effectively extinct in thermal transport, contributing negligibly to the thermal conductivity. The extinction of high-frequency phonons explains the clear reduction in the growth rate of κ with length beyond 69.5 nm in Fig. 2. However, the overall thermal conductivity still increases monotonically with length, because low-frequency phonons remain nearly ballistic and continue to dominate transport. As a result, the system does not exhibit the nonmonotonic decay of thermal conductivity expected from Anderson localization, despite the loss of mid- and high-frequency contributions.

When correlation is introduced ($a = 1$), the transmission of low-frequency phonons is already slightly suppressed at short lengths ($L = 17.4$ nm) compared to the random case, whereas high-frequency phonon transmission is marginally enhanced. As the length increases, this trend becomes more pronounced: low-frequency modes ($\omega < 2$ THz) are significantly suppressed, signaling the phonon localization, while the transmission of high-frequency phonons remains finite up to longer distances before ultimately decaying. Meanwhile, the suppression of scattering at high frequencies allows these modes to persist over longer distances. The mode-selective localization has a nontrivial impact on heat transport. The suppression of low-frequency phonons, which are typically the most effective heat carriers, drastically reduces the thermal conductivity. While the increased high-frequency transmission partially compensates for this loss at intermediate lengths, these modes eventually attenuate in long nanowires, leading to an overall decline in κ with increasing L. This mechanism explains the nonmonotonic behavior and the appearance of a thermal conductivity maximum in correlated systems, which is an effect absent in purely random disorder.

Furthermore, figures 5(d)–5(f) further compare the transmission between $a = 0.1$ correlated and randomly disordered systems. As correlation strengthens (a decreases), we observe a further reduction in low-frequency transmission and a more pronounced enhancement in the high-frequency range, particularly between 4–8 THz. This reinforces the mode-selective nature of correlation-induced localization: stronger correlations enhance interference-driven backscattering for low-frequency modes, while simultaneously reducing high-frequency scattering due to smoother spatial variation. Correlation does not simply shift or smooth the disorder landscape, but instead fundamentally restructures phonon transport by reshaping the transmission spectrum. This results in a regime where thermal transport is dominated not by scattering strength, but by the spectral redistribution of localization effects, which are selectively amplified by correlation.

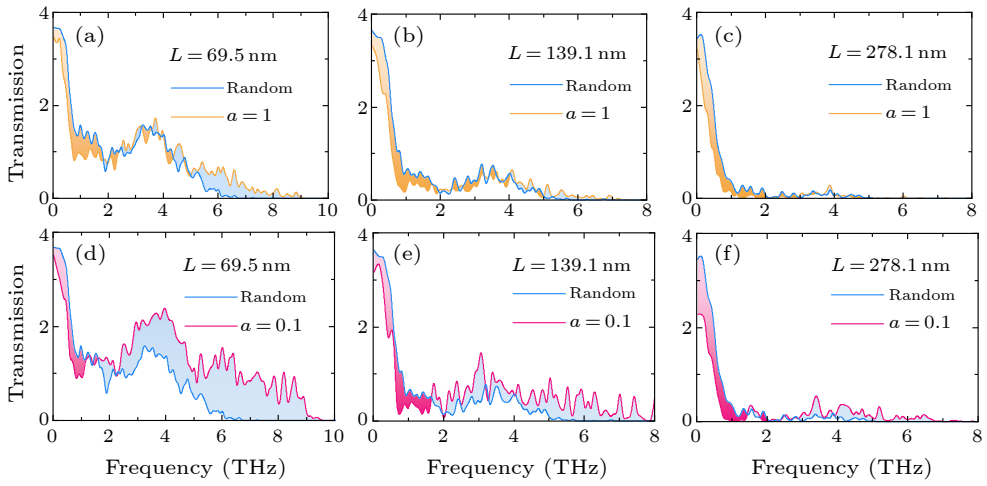

Fig. 5. Full-spectrum phonon transmission: (a)–(c) $a = 1$ vs. random; (d)–(f) $a = 0.1$ vs. random. Each column corresponds to $L = 69.5$, 139.1, and 278.1 nm, respectively.

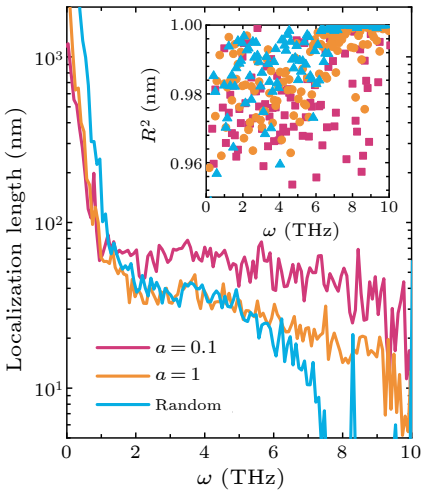

Fig. 6. Localization length $\xi(\omega)$ for nanowires with different disorder types. Inset: Corresponding fitting R^2 values, which indicate the fit quality of localization length.

To provide a quantitative understanding of how correlation affects phonon localization across the entire frequency spectrum, we extract the frequency-resolved localization length $\xi(\omega)$ by fitting the phonon transmission $\mathcal{T}(\omega, L)$ across different sample lengths to an exponential decay,

$$\mathcal{T}(\omega, L) = \mathcal{T}_0(\omega) \exp[-L/\xi(\omega)], \tag{6}$$

where $\mathcal{T}_0(\omega)$ corresponds to the transmission of the shortest nanowire with a length of 2.2 nm. The fitting was carried out using NEGF-calculated transmission data over a series of 10 nanowire lengths ranging from 4.3 to 278.1 nm. The quality of the exponential fits was quantified by the coefficient of determination R^2, as shown in the inset of Fig. 6. Values with $R^2 > 0.95$ were considered to be reliable for the fitting and were used to extract the reported $\xi(\omega)$. With standard NEGF-based localization analyses,[28,32,33,37] we are able to extrapolated $\xi(\omega)$ values much larger than the maximum system length considered. This feature allows the extrapolation of ξ for the low-frequency modes, which possess very long mean free paths[33,34] and consequently large ξ values.

Figure 6 presents the resulting localization lengths for disordered Si-like nanowires with random mass distribution and two correlated disorder cases with $a = 1$ and $a = 0.1$. The inset shows the corresponding coefficient of determination R^2 for each frequency, confirming that most fits yield reliable localization lengths. In the low-frequency regime ($\omega < 2$ THz), random disorder exhibits the longest localization lengths, with $\xi(\omega)$ exceeding 200 nm at sub-THz frequencies. However, introducing correlation significantly reduces $\xi(\omega)$ in this regime. In particular, for the strongly correlated case ($a = 0.1$), the localization length drops by nearly an order of magnitude below 1 THz, which clearly indicates that correlation enhances the localization of low-frequency phonons, despite the fact that it reduces the number of mass interfaces.

In the intermediate frequency range (2–6 THz), the localization behavior differentiates the two correlated cases. The weakly correlated structure ($a = 1$) exhibits localization lengths comparable to the random case. In contrast, the $a = 0.1$ case shows noticeably higher $\xi(\omega)$ in this range, frequently exceeding 70 nm, which suggest that strong correlation delays localization for these mid-frequency modes. This activation of intermediate-frequency phonons compensates for the loss of low-frequency carriers and explains the initial enhancement in thermal conductivity observed in correlated systems of moderate length. At high frequencies ($\omega > 6$ THz), all three disorder types result in short localization lengths ($\xi < 30$ nm), reflecting the strong scattering and rapid localization of high-frequency phonons. Nevertheless, the $a = 0.1$ case consistently maintains slightly larger $\xi(\omega)$ compared to the other two, implying that strongly correlated structures provide partial pathways for high-frequency modes to contribute to thermal transport before complete localization sets in.

4. Conclusion. In summary, we investigated phonon transport in silicon-like nanowires with spatially correlated mass disorder using the NEGF method. We found that such correlations induce nonmonotonic thermal conductivity behavior with length, in contrast to the monotonic increase observed in random disorder. Correlated systems exhibit lower thermal conductivity at large lengths, a phenomenon attributed to the enhanced localization of low-frequency phonons, even though they contain fewer mass interfaces. Meanwhile, mid- and high-frequency phonon modes benefit from smoother mass variation, experiencing partial delocalization. Frequency-resolved analysis reveals that spatial correlation reshapes the spectrum of thermally active phonons, promoting coherent backscattering. Our study highlights disorder correlation as a key design parameter for tailoring phonon transport in low-dimensional systems, with implications for thermal management and phononic device engineering.

Acknowledgements. This work was supported by the National Natural Science Foundation of China (Grant Nos. U22A20210, 52576070 for H. Y.; and 12174276 for S. X.), the Basic and Applied Basic Research Foundation of Guangdong Province (Grant No. 2024A1515010521 for S. X.), and the China Scholarship Council (CSC) (Grant No. 202406120152 for W. Z.).

References

[1] Xu Q, Zhou J W, Liu T H, and Chen G 2021 *Phys. Rev. Appl.* **16** 064052
[2] Lim J, Wang H T, Tang J Y, Andrews S C, So H Y, Lee J, Lee D H, Russell T P, and Yang P D 2016 *ACS Nano* **10** 124
[3] Qian X, Zhou J W, and Chen G 2021 *Nat. Mater.* **20** 1188
[4] Huang X, Anufriev R, Jalabert L, Watanabe K, Taniguchi T, Guo Y Y, Ni Y X, Volz S, and Nomura M 2024 *Nature* **634** 1086
[5] Li N B, Ren J, Wang L, Zhang G, Hänggi P, and Li B 2012 *Rev. Modern Phys.* **84** 1045
[6] Kasprzak M, Sledzinska M, Zaleski K, Iatsunskyi I, Alzina F, Volz S, Sotomayor T C M, and Graczykowski B 2020 *Nano Energy* **78** 105261
[7] Chang C W, Okawa D, Garcia H, Majumdar A, and Zettl A 2008 *Phys. Rev. Lett.* **101** 075903

[8] Yang N, Zhang G, and Li B W 2010 *Nano Today* **5** 85
[9] Zhang Z W, Ouyang Y L, Cheng Y, Chen J, Li N B, and Zhang G 2020 *Phys. Rep.* **860** 1
[10] Anufriev R, Yanagisawa R, and Nomura M 2017 *Nanoscale* **9** 15083
[11] Li W K, Zhang W T, Huang X Y, Mu X, and Ni Y X 2024 *Int. J. Heat Mass Transfer* **220** 124955
[12] Neogi S and Donadio D 2020 *Phys. Rev. Appl.* **14** 024004
[13] Honarvar H and Hussein M I 2018 *Phys. Rev. B* **97** 195413
[14] Yang L N and Hussein M I 2024 *J. Phys.: Condens. Matter* **36** 505303
[15] Wan X, Ma D K, Pan D K, Yang L N, and Yang N 2021 *Mater. Today Phys.* **20** 100445
[16] Diego M, Hardouin J, Mazevet-Schargrod G, Pirro M, Kim B, Anufriev R, and Nomura M 2025 *Sci. Adv.* **11** eadw7205
[17] Huang X Y, Volz S, Nomura M, and Ni Y X 2025 *Phys. Rev. B* **111** 174203
[18] Hu S Q, Zhang Z W, Jiang P F, Chen J, Volz S, Nomura M, and Li B W 2018 *J. Phys. Chem. Lett.* **9** 3959
[19] Yang L N, Latour B, and Minnich A J 2018 *Phys. Rev. B* **97** 205306
[20] Yang L N, Yang B S, and Li B W 2023 *Phys. Rev. B* **108** 165303
[21] Pirie H, Sadhuka S, Wang J, Andrei R, and Hoffman J E 2022 *Phys. Rev. Lett.* **128** 015501
[22] Zhang T T, Liu Y Z, Miao H, and Murakami S 2025 arXiv:2505.06179 [cond-mat.mtrl-sci]
[23] Anderson P W 1958 *Phys. Rev.* **109** 1492
[24] Sheng P 2006 *Introduction to Wave Scattering, Localization, and Mesoscopic Phenomena* 2nd ed (Berlin, New York: Springer)
[25] Cui L, Wei G S, Li Z, and Du X Z 2021 *Int. J. Heat Mass Transfer* **165** 120685
[26] Burkov S E, Koltenbah B E C, and Bruch L W 1996 *Phys. Rev. B* **53** 14179
[27] Shi W W and Tong P Q 2023 *Phys. Rev. B* **108** 024202
[28] Juntunen T, Vänskä O, and Tittonen L 2019 *Phys. Rev. Lett.* **122** 105901
[29] Hu R J and Tian Z T 2021 *Phys. Rev. B* **103** 045304
[30] Guo Y Y, Bescond M, Zhang Z W, Xiong S Y, Hirakawa K, Nomura M, and Volz S 2021 *APL Mater.* **9** 091104
[31] Ni Y X, Huang X Y, Zhai F Y, Chen Y Z, Wang H Y, and Zhang H G 2024 *J. Appl. Phys.* **135** 095108
[32] Mendoza J and Chen G 2016 *Nano Lett.* **16** 7616
[33] Luckyanova M N, Mendoza J, Lu H, Song B, Huang S, Zhou J, Li M, Dong Y, Zhou H, Garlow J, Wu L, Kirby B J, Grutter A J, Puretzky A A, Zhu Y, Dresselhaus M S, Gossard A, and Chen G 2018 *Sci. Adv.* **4** eaat9460
[34] Zhang W, Guo Y Y, Xiong S Y, and Yi H L 2023 *Phys. Rev. B* **108** 125436
[35] Mondal W R, Vidhyadhiraja N S, Berlijn T, Moreno J, and Jarrell M 2017 *Phys. Rev. B* **96** 014203
[36] Yamamoto T, Sasaoka K, and Watanabe S 2011 *Phys. Rev. Lett.* **106** 215503
[37] Savić L, Mingo N, and Stewart D A 2008 *Phys. Rev. Lett.* **101** 165502
[38] Roy C P, Reynolds C, Garrett A, Feng T L, Adiga S P, and Ruan X L 2020 *Nano Energy* **69** 104428
[39] Makse H A, Havlin S, Schwartz M, and Stanley H E 1996 *Phys. Rev. E* **53** 5445
[40] Fiorentino A, Pegolo P, Baroni S, and Donadio D 2025 *Phys. Rev. B* **111** 134205
[41] Thébaud S, Lindsay L, and Berlijn T 2023 *Phys. Rev. Lett.* **131** 026301
[42] Fricke N, Zierenberg J, Marenz M, Spitzner F P, Blavatska V, and Janke W 2017 *Condens. Matter Phys.* **20** 13004
[43] Zierenberg J, Fricke N, Marenz M, Spitzner F P, Blavatska V, and Janke W 2017 *Phys. Rev. E* **96** 062125
[44] Tersoff J 1989 *Phys. Rev. B* **39** 5566
[45] Landauer R 1957 *IBM J. Res. Dev.* **1** 223
[46] Landauer R 1970 *Philos. Mag.* **21** 863
[47] Imry Y and Landauer R 1999 *Rev. Mod. Phys.* **71** S306
[48] Hu M, Zhang X L, Giapis K P, and Poulikakos D 2011 *Phys. Rev. B* **84** 085442